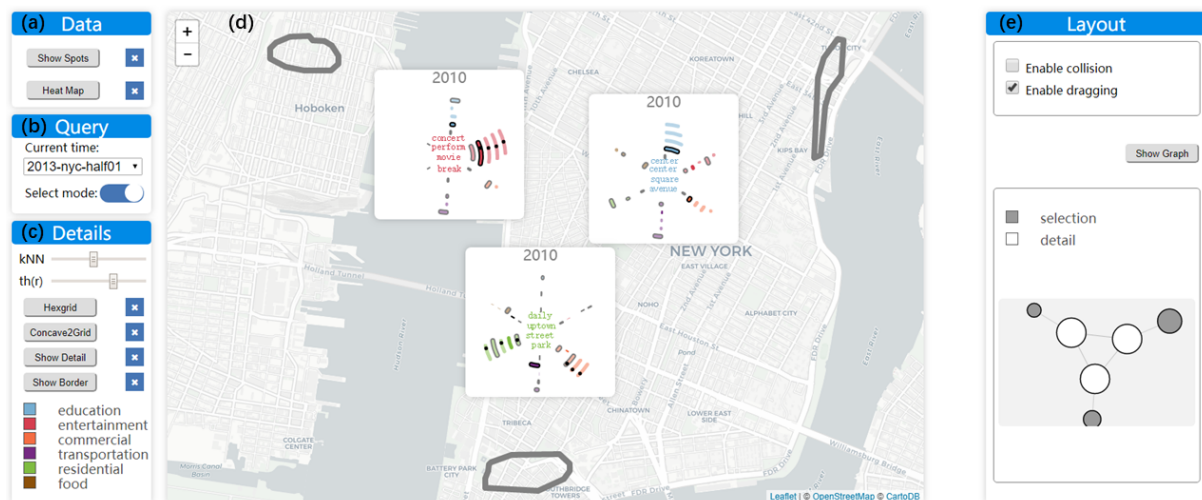


# Visualizing Functional Regions by Analysis of Geo-textual Data

Yunzhe Wang<sup>1</sup>, George Baciu<sup>1</sup> and Chenhui Li<sup>2</sup>

<sup>1</sup>The Hong Kong Polytechnic University

<sup>2</sup>East China Normal University



**Figure 1:** The interface of our system consists of (a) Data menu. Scatter plot and heatmap are provided for displaying the the distribution of data. (b) Query menu. Users can retrieve data at specific time, or enable the free selection mode to query an AOI (Area Of Interest). (c) The Details menu allows users to change parameters, view details of AOIs and refer the color legend. (d) Map view of the current time step. (e) In the Layout menu, users can adjust positions of details.

## Abstract

Using tremendous geo-textual data collected from social media applications, we facilitate the analysis of region functions. By extracting semantics from textual properties, we aim at classifying geographical locations in terms of their functional types. Hence, we train a classification model with the Support Vector Machine, and apply it to aggregated word embeddings to predict the function of spots. We highly cooperate with techniques in graph analysis. Firstly, regions are segmented based on a latent graph. Then, we propose an adaptive layout solution to deal with situations of multi-AOI queries. The generated layout and interactive metaphor provide convenience for observation and comparison. Experiments are conducted with the YFCC100M dataset to prove the effectiveness of our system.

## CCS Concepts

•Human-centered computing → Visual analytics;

## 1. Introduction

The interplay between human activities and dynamics of regions affect decisions of various issues, including urban planning, commercial development and maintenance of social order. Regions such as food court, CBD and residential communities provide specific fa-

cilities so that people within them tend to perform similar type of activities.

Functional division provides a legible understanding of the city composition. Analysts gain insights into the geographical distribution and the influence of various functional regions. Some regions

are highly dynamic. Their territories might expand or shrink, and the inner functions even change. Normally, on-spot investigation is not practical. Most of the existing work explores human movements to divide regions. However, mobility data are typically obtained from transportation tools like taxi and metro, which cannot provide a full coverage of focal areas. Besides, the interpretation of region functions still relies on prior knowledge.

Recently, the geo-textual data burst with the prevalence of social media. On photo-sharing platforms, users can record geo-positions (i.e., *spots*) where photos were taken. They are allowed to attach descriptive texts which imply contexts of the spots. We propose to cluster spots using a graph-based method. Each cluster is regarded as a *region*. After inspecting all inner spots, we find that some regions have *explicit* functions, while others possess a mixture of functions. The contributions of our work are as follows,

- We reduce the feature diversity of geo-locations by classifying semantics extracted from geo-textual data. Semantics are represented by aggregating embeddings of representative words.
- Regions are segmented by maximizing the modularity of a latent graph. The graph integrates both spatial and functional proximity. Therefore, closely located spots with similar context constitute a region.
- Instead of creating a separate view, we place AOI details on the map and optimize their positions. By mapping AOIs and details to nodes in a graph, force layout method can be applied to ensure that the detail position is close to the corresponding AOI and to all other details of remaining AOIs simultaneously.

## 2. Related Work

Region segmentation can be achieved by recognizing different patterns of human activities. People tend to perform similarly within a region. Cranshaw et al. [CSHS12] counted the visiting frequency of a location by all users, and locations of similar visiting patterns are placed into the same region. This work lacks the interpretation of region functions. Main roads can be treated as a reference for segmentation. Yuan et al. [YZX\*15] used POI statistics and a topic model to infer region functions. However, their method cannot further divide a large region, due to the limitation of road network. MobiSeg [WZC\*17] supports dynamic updating of region segmentation, which is based on a tessellation procedure. Data from multiple sources are fused to mitigate the sparsity problem. Interestingly, both work of Wu et al. [WZC\*17] and Yuan et al. [YZX\*15] proposed analogies to the context of textual analysis, while our work directly manipulates the textual data.

Extensive research has been conducted to uncover the functions of regions, also known as the land use. Previous studies took remote-sensing satellite images as input and get results at a coarse level. Voorde et al. [VdVJC11] classified areas in terms of residential, commercial, service and green space. To attain fine-grained categories, supervised classification methods as adopted by Pan et al. [PQW\*13] need to be applied. We carried out a similar work, except that their training set contains regions and manually labeled functions, while our training set consists of spot-function pairs. We believe that it is more reasonable to classify spots, because some regions may have several functions involved. Hence, it is not easy to decide a specific function to label them.

In natural language processing, word embedding aims at converting a word to a numeric vector for further operations like classification and regression. Short text semantics may reflect features of geo-locations and also help to support situational assessment [MJR\*11].

Many visual analytic systems for geographical data prefer to put details that users query in a separate view, mostly because they want to provide organized views to facilitate comparisons. Wu et al. [WZC\*17] place the mobility feature vectors of local districts in a detail view. However, users have to switch between two views to map their queries and corresponding details. Yang et al. [YDGM17] use a leader line to connect locations with visualizations. To decide optimal locations for billboards, multiple solutions of the target area are provided in SmartAdP [LWL\*17]. In this work, we place details next to queried areas to relieve users from mapping.

## 3. Method

### 3.1. Data Format

We conducted experiments on the YFCC100m dataset [TSF\*16]. Especially, we focus on data of New York City, and we aggregate data by half of a year. For each data item, we filtered 9 attributes, (*user\_id, time, upload\_time, title, description, tag, longitude, latitude, url*), where *time* is when the photo was taken. *title, description* and *tag* describe content in the photo. Original texts of the three attributes might involve random characters and stop words, so we clean them and only preserve meaningful English words. In the end, a spot *i* associates with a list of words,  $W_i = \{w_1, w_2, \dots, w_k\}$ . *longitude, latitude* give the position where the photo was taken. We can access the photo through the *url* attribute.

### 3.2. Spot Semantics

The function of a region is revealed by investigating the characteristics of its inner spots. We get spot (e.g., *i*) features by analyzing semantics of the corresponding word list (e.g.,  $W_i$ ). Hence, we can deduce if the place is famous for food, tourism, or commerce. First of all, we adopt Word2Vec [MCC\*14] to project words into a vector space. The distributed representations [MSC\*13] generated by Word2Vec embed rich context information. For training, we input a corpus of 3 million words. Finally, a word  $w_j$  can be represented by a 300-dimensional vector,  $v_j = [f_1, f_2, \dots, f_{300}]$ .

As a spot might associate with a list of words, its semantics  $S_i$  can be described by aggregating vectors of words in  $W_i$ .

$$S_i = g([t_1, t_2, \dots, t_k] \begin{bmatrix} v_1 \\ v_2 \\ \dots \\ v_k \end{bmatrix}), \quad (1)$$

where  $g(\cdot)$  is an aggregation operator, which can be min/max, or mean of each dimension in word vectors [DBVCDD16]. In this work, we adopt the max operator. Each vector (i.e.,  $v_j$ ) is weighted by the TF-IDF value (i.e.,  $t_j$ ) of word (i.e.,  $w_j$ ),  $t_j = \frac{n_{ji}}{\sum_k n_{kj}} \times \log \frac{|P|}{|\{i: w_j \in p_i\}|}$ , where  $n_{ji}$  denotes the frequency that  $w_j$  occurs in  $W_i$ ;  $\sum_k n_{kj}$  is the sum of all word frequencies in  $W_i$ ;  $|P|$  is the

number of posts in one time step, and the denominator in IDF is the number of posts which contain the word  $w_j$ .

Our ultimate goal is to classify spots into different types. Therefore, we trained a classification model which is based on SVM and a RBF kernel. In the training set, each spot is manually labeled with an appropriate type. In this work, we have six types [residential, commercial, transportation, food, education, entertainment]. Namely, spot  $i$  can be represented by  $[S_i, T_i]$  in the training set, where  $T_i$  is one of the six types. Functions of all other spots are then predicted by the classification model.

### 3.3. Region Segmentation

To divide a whole area into regions, we hope to find spots that are both closely located and are of similar semantics. We construct a graph  $G$  in which a spot connects to its  $k$  Nearest Neighbors (kNN) according to their haversine distances. The connection weight  $E_{ij} = \frac{S_i \cdot S_j}{\|S_i\| \|S_j\|}$  is the cosine distance between semantic vectors of two end spots  $i$  and  $j$ , which reflects the semantic similarity.

Then, we conduct Community Detection on  $G$  by maximizing the modularity [RSC\*10], which is defined as

$$Q = \frac{1}{2m} \sum_{uv} \left[ A_{uv} - \frac{k_u k_v}{2m} \right] \frac{s_u s_v + 1}{2}, \quad (2)$$

where  $u$  and  $v$  are nodes in the graph;  $A$  is the adjacency matrix;  $k_u$  is the degree of node  $u$  and  $s$  indicates the membership of a node to community. In this way, spots are separated into disjoint communities. We take the geographical coverage of a community as a region, and the boundary is regarded as the concave hull of spots. The function type of a region is decided according to statistics of inner spots. Details are given in Section 4.

### 3.4. Visualization

To let users fully explore the functional regions, our analytic system is required to provide following utilities: (1) showing the distribution of spots, (2) allowing free query on both spatial and temporal dimensions, (3) reducing the diversity of semantics and project them to comprehensive visual space, and (4) facilitating visual comparisons of region territories and statistics. Here, we emphasize three significant aspects of our visual design.

Firstly, for the benefit of aesthetic perception [CCW\*16] and easy comparison, we convert concave polygons to conjoint hexagon cells. Since original polygons are in irregular shapes, it is difficult to visually compare the size of different regions. After conversion, the region coverage can be denoted by the number of hexagon cells that it contains, because all cells are in uniform size. As shown in Figure 5, we spread a hexagon grid onto the focal area. Then, Scan-line method [WREE67] is used to check all cells in the grid. By applying the ray casting method [Rot82], we detect cells intersected with polygons.

Secondly, users are allowed to freely select an Area Of Interest (AOI). By clicking the AOI border, a scalable metaphor which encodes temporal details will display on the map. As shown in Figure 2, each ring consists of categorical data at one time step. From the inside out, rings are placed following a chronological order.

Generally, space is uniformly divided by hidden axes into 6 sections. Arcs of a certain category are aligned along the axis. The arc length  $l$  is calculated by  $l = N_t * (1/6 * 2\pi * r) / N$ .  $N_t$  is the number of spots of type  $t$  and  $N$  is the total number of spots.  $r$  denotes the radius of the ring. To reveal the evolution, an arc is encompassed with a black border, if  $N_t/N$  becomes larger. We also preserve a circular space in the center to represent popular keywords of the dominant function. The black dot shows the existence of explicit regions. The arc length from the axis to the dot indicates the ratio of spots belonging to the explicit region.

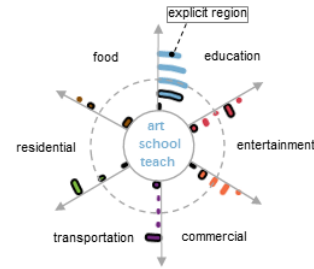


**Figure 2:** A multi-ring metaphor shows temporal details of an AOI. Each ring shows data of one time step (e.g., the dashed ring denotes the third step). Hidden axes equally divide space into 6 sections, corresponding to 6 function types. The length of an arc indicates the proportion of spots of a certain type. If the proportion grows, the arc is highlighted with a black border. A black dots implies an explicit region. Keywords of the most dominant function locate in the central circular space.

Thirdly, when users select several AOIs and compare their details, we utilize force layout algorithms [Dwy09] to decide the layout of details. We abstract AOIs and details as nodes, which are depicted by their smallest enclosing circles. We want a detail metaphor to stay as close as possible to the related AOI, so that users do not need to take a long eye movement for mapping. Besides, all details should get close to facilitate the comparison. Hence, we connect each AOI with the corresponding details, and all details are fully connected. As AOIs are fixed, the force layout algorithm outputs optimal positions of details.

## 4. Experiment

To evaluate our system, we retrieve all posts in New York city during 2009 to 2014. Time interval is set to half a year. Users might take several photos at a spot and no textual information added. Results in this section are based on data in the first half of year 2013, where 10406 identical spots contribute to region segmentation.

The interface contains five parts, as shown in Fig. 1. Figure 3 displays the spot distribution in two ways. Clicking a spot allows users to access the photo. Heatmap helps users to locate a potential AOI by density. We also found that explicit regions are more likely to lie in high density areas.

Each spot is connected to its 10 nearest neighbors. Figure 4(a) presents the resulted graph. Communities are detected on such a graph and they delimit by bounding spots of a community with a

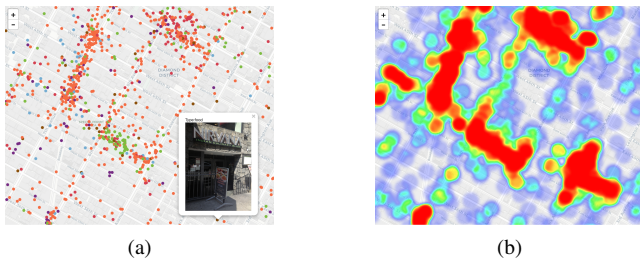


**Figure 3:** Partial distribution of data in the first half of year 2013 in NYC. (a) In the scatter plot, spots are filled with different colors to show their functional types after classification. (b) Heatmap signifies high density areas with warmer colors.

concave polygon, as shown in Fig. 4(b). The average number of spots at all time steps is 15978, and the average time of community detection is 0.6802 seconds. A region is *explicit* if over 70% of spots have the same function. However, as shown in Fig. 5, only a few of them are *explicit*. It implies that many regions in NYC have no dominant function and they integrate with multiple functions. In explicit regions, only one type dominates. For instance, R1 in Fig. 5 turns out to be the Metropolitan Museum of Art, which is defined as *education* related.



**Figure 4:** Cluster spots based on kNN graph. (a) Graph constructed by connecting spots with its 10NN neighbors. (b) Communities are delimited by concave boundaries.

In this work, the width of hexagon cells is 100 meters. In Fig. 5, we convert all *explicit* regions into combinations of hexagon cells. In NYC, many regions are commercial related (i.e., regions filled with *orange*). In our definition, all themes about shopping, business, finance are categorized as commercial. Most of these regions locate in the center of NYC. After conversion, regions close to each other merge together, such as R2 in Fig. 5. Actually, we can see that R2 stretches along the Fifth Avenue, which is known as one of the most expensive shopping streets in the world.

Two cases in Fig. 6 show how our system can adaptively place details on the map. Users can get rid of one-to-one mappings between two separate views. Because a detail metaphor is placed next to the related AOI. All metaphors stay as close as possible to facilitate comparisons between different AOIs. When users hover around, all arcs at the same time step will be highlighted.

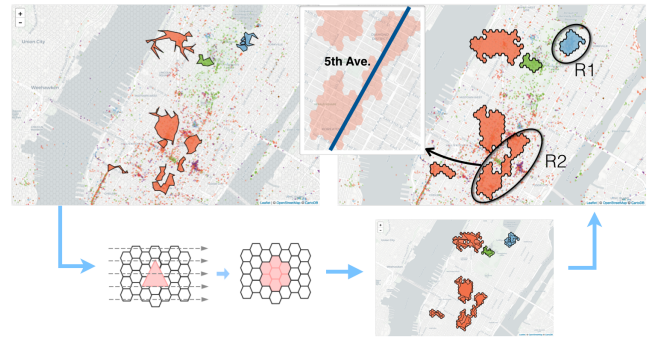


**Figure 5:** Convert concave polygons to hexagon cells. Polygons represent explicit regions, based on results of community detection. By applying the ScanLine and ray casting methods, all cells intersected with the polygon will be filled with the same color.



**Figure 6:** Given positions of AOIs selected by users, our system can adaptively put detail views around them. Sub-figures in the top-left corner show thumbnails of the layout. Grey nodes and white nodes denote AOIs and details respectively. Five AOIs (a) far from each other. (b) close to each other.

## 5. Conclusions

In this work, we segment regions by clustering similar spots in terms of semantics of corresponding textual data. To decide if a region has an explicit function, we inspect all inner spots. In our visual system, users can observe the overall distribution of all explicit regions, or they can query an AOI and view the temporal evolution. However, there still exist several open issues. For example, the classification accuracy of textual semantics needs to be improved. For the future work, we can calibrate the accuracy by analyzing image contents, which are especially useful when no meaningful textual data are available. Another issue is that the adaptive visual mapping is not scalable enough and we now assume that users will not query more than 10 AOIs at one time. Also, we need to conduct user studies to evaluate the performance of our visual analytic system.

## Acknowledgements

The authors would like to acknowledge the partial support of IGRF PolyU 152142/15E and Project 4-ZZFF from the Department of Computing, The Hong Kong Polytechnic University.

## References

- [CCW\*16] CHEN S., CHEN S., WANG Z., LIANG J., YUAN X., CAO N., WU Y.: D-map: Visual analysis of ego-centric information diffusion patterns in social media. In *Visual Analytics Science and Technology (VAST), 2016 IEEE Conference on* (2016), IEEE, pp. 41–50. 3
- [CSHS12] CRANSHAW J., SCHWARTZ R., HONG J. I., SADEH N.: The livelihoods project: Utilizing social media to understand the dynamics of a city. 2
- [DBVCDD16] DE BOOM C., VAN CANNEYT S., DEMEESTER T., DHOEDT B.: Representation learning for very short texts using weighted word embedding aggregation. *Pattern Recognition Letters* 80 (2016), 150–156. 2
- [Dwy09] DWYER T.: Scalable, versatile and simple constrained graph layout. In *Computer Graphics Forum* (2009), vol. 28, Wiley Online Library, pp. 991–998. 3
- [LWL\*17] LIU D., WENG D., LI Y., BAO J., ZHENG Y., QU H., WU Y.: Smartadp: Visual analytics of large-scale taxi trajectories for selecting billboard locations. *IEEE transactions on visualization and computer graphics* 23, 1 (2017), 1–10. 2
- [MCC\*14] MIKOLOV T., CHEN K., CORRADO G., DEAN J., SUTSKEVER L., ZWEIG G.: word2vec, 2014. 2
- [MJR\*11] MACEACHREN A. M., JAISWAL A., ROBINSON A. C., PEZANOWSKI S., SAVELYEV A., MITRA P., ZHANG X., BLANFORD J.: Senseplace2: Geotwitter analytics support for situational awareness. In *Visual Analytics Science and Technology (VAST), 2011 IEEE Conference on* (2011), IEEE, pp. 181–190. 2
- [MSC\*13] MIKOLOV T., SUTSKEVER I., CHEN K., CORRADO G. S., DEAN J.: Distributed representations of words and phrases and their compositionality. In *Advances in neural information processing systems* (2013), pp. 3111–3119. 2
- [PQW\*13] PAN G., QI G., WU Z., ZHANG D., LI S.: Land-use classification using taxi gps traces. *IEEE Transactions on Intelligent Transportation Systems* 14, 1 (2013), 113–123. 2
- [Rot82] ROTH S. D.: Ray casting for modeling solids. *Computer graphics and image processing* 18, 2 (1982), 109–144. 3
- [RSC\*10] RATTI C., SOBOLEVSKY S., CALABRESE F., ANDRIS C., READES J., MARTINO M., CLAXTON R., STROGATZ S. H.: Redrawing the map of great britain from a network of human interactions. *PLoS one* 5, 12 (2010), e14248. 3
- [TSF\*16] THOMEE B., SHAMMA D. A., FRIEDLAND G., ELIZALDE B., NI K., POLAND D., BORTH D., LI L.-J.: Yfcc100m: The new data in multimedia research. *Communications of the ACM* 59, 2 (2016), 64–73. 2
- [VdVJC11] VAN DE VOORDE T., JACQUET W., CANTERS F.: Mapping form and function in urban areas: An approach based on urban metrics and continuous impervious surface data. *Landscape and Urban Planning* 102, 3 (2011), 143–155. 2
- [WREE67] WYLIE C., ROMNEY G., EVANS D., ERDAHL A.: Half-tone perspective drawings by computer. In *Proceedings of the November 14-16, 1967, fall joint computer conference* (1967), ACM, pp. 49–58. 3
- [WZC\*17] WU W., ZHENG Y., CAO N., ZENG H., NI B., QU H., NI L. M.: Mobiseg: Interactive region segmentation using heterogeneous mobility data. In *Pacific Visualization Symposium (PacificVis), 2017 IEEE* (2017), IEEE, pp. 91–100. 2
- [YDGM17] YANG Y., DWYER T., GOODWIN S., MARRIOTT K.: Many-to-many geographically-embedded flow visualisation: an evaluation. *IEEE transactions on visualization and computer graphics* 23, 1 (2017), 411–420. 2
- [YZX\*15] YUAN N. J., ZHENG Y., XIE X., WANG Y., ZHENG K., XIIONG H.: Discovering urban functional zones using latent activity trajectories. *IEEE Transactions on Knowledge and Data Engineering* 27, 3 (2015), 712–725. 2